

NUCLEAR
INSTRUMENTS
& METHODS
IN PHYSICS
RESEARCH

Multi-bundle shashlik calorimeter prototypes beam-test results

RD-36 Collaboration

J. Badier ^a, Ph. Bloch ^g, S. Bityukov ^b, P. Bordalo ^c, Ph. Busson ^a, C. Charlot ^a, L. Dobrzynski ^{a,*}, I. Golutvin ^e, S. Gninenko ^d, E. Guschin ^d, V. Issakov ^d, I. Ivanchenko ^e, V. Lapshin ^b, V. Klimenko ^d, V. Marin ^d, P. Moissenz ^e, Y. Musienko ^d, V. Obraztsov ^b, A. Ostankov ^b, V. Popov ^c, I. Puljak ^h, S. Ramos ^c, C. Seez ^f, S. Sergueev ^e, I. Semenyuk ^d, V. Soushkov ^b, R. Tanaka ^a, J. Varela ^c, T.S. Virdee ^f, A. Zaitchenko ^b, N. Zamiatin ^e

^a LPNHE-Ecole Polytechnique, IN2P3-CNRS, Palaiseau, France

^b IHEP, Protvino, Russian Federation

^c LIP, Lisbon, Portugal

^d INR, Moscow, Russian Federation

^c JINR, Dubna, Russian Federation

^f Imperial College, London, UK

^g CERN, Geneva, Switzerland

^h FESB, University of Split, Split, Croatia

Received 22 July 1994

Abstract

The first beam-test results for two- and three-bundle shashlik tower prototypes are described. We found that the spatial resolution, the uniformity of energy response, the calorimeter reliability and hermeticity and also two showers separation are improved in multi-bundle design approach.

1. Introduction

The "shashlik" calorimeter, is a lead-scintillator sandwich sampling calorimeter readout by Wave Length Shifter (WLS) fibres. It is the baseline option for the electromagnetic calorimeter for the CMS experiment at LHC [1,2]. Under development for the last 10 years [3] this type of calorimeter should satisfy the main requirements for LHC experiments: high rate capability, compactness, rather good energy and spatial resolution, etc. [2,4]. The main advantage of such calorimeter type is the much lower cost in comparison with a homogenous (total absorption) calorimeter. The cost is essentially defined by high precision machining of lead and scintillator tiles, which is necessary for high hermeticity and uniformity. Hence the total cost of such a calorimeter depends mostly on the number of towers and much less on its volume. On the other side, the calorimeter cell size should be small enough

2. Multi-bundle tower design

Among the "shashlik" prototype projective towers [6] tested at CERN in 1993 two towers were manufactured as shown in Fig. 1. The fibres, collected in bunches, share the light signal from calorimeter tiles, leading to two (tower 16) and three (tower 15) readout cells in one single tower. The separation of fibres is done in one direction. A more precise coordinate measurement in pseudorapidity is required for the CMS experiment. Since all the fibres in one tower capture light from the same scintillator tiles, a point light source will give rise to a signal in all channels. This may be considered as a cross talk between readout channels. However, its value depends on the light source position so it can be used for coordinate measurements as it was shown in Ref. [5]. A drawback may be the increased

to provide the required spatial resolution and low pileup noise. As a compromise, the following variant of a multibundle tower design is proposed and has been tested.

^{*} Corresponding author, Email: dobj@frcpn11.

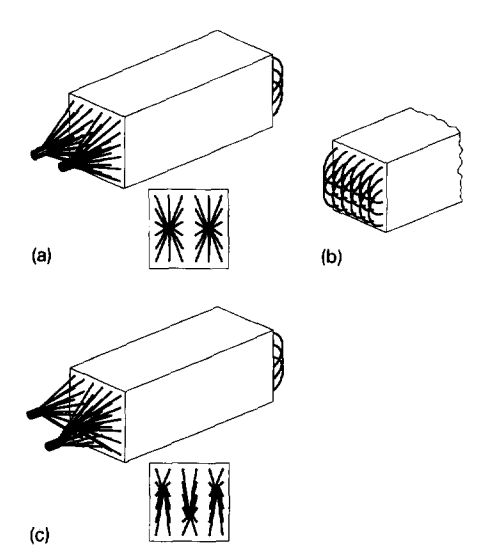


Fig. 1. The multi-bundle "shashlik" towers design. (a) Tower 16, (b) front view, (c) Tower 15.

pileup noise. More simulation studies are still necessary to define the final dimension of towers for LHC experimental conditions.

The present towers were of projective pointing geometry with square cross section. The dimension of the front face of the towers was 52.5 mm and the rear face size was about 64 mm. The fibres used had a diameter of 1.2 mm. They run parallel to each other and to the tower axis and are placed in a 6×6 matrix with distance between fibres of 9.5 mm. Tower 15 (three bundles) was equipped with Y-7 type of fibres. Tower 16 has K-27 fibres. It was found that Cherenkov and/or direct scintillation light is larger in Y-7 fibres than in the K27 ones.

3. Experimental setup

The program of test measurements was performed in the SPS-H2 test beam at CERN. It consisted of a coordinate scan with 40 GeV electrons beam in the horizontal plane at the middle of the tower. The tower to be tested,

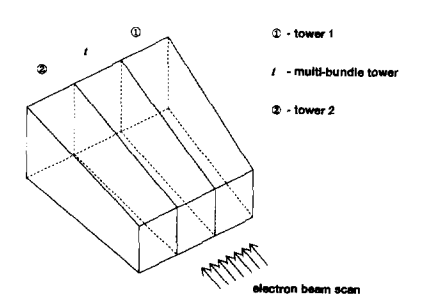


Fig. 2. Experimental setup. Horizontal coordinate scan at tower median with 40 GeV electrons.

marked by "t" in Fig. 2 was located between two towers. The tower axis was parallel to the beam. The scan was performed with a 20×20 mm² beam spot size. Data for the central tower were taken at 7 points with a step of 10.5 mm between points. The number of events taken for each beam position was about 5000. Beam particle coordinate was measured by two delay line wire chamber with an accuracy of 300 μ m.

4. Tower readout

To detect the light from WLS fibres, Hamamatsu-3590-05 Si-photodiodes equipped with low noise hybrid preamplifiers [7] were used. The photodiode sensitive area was 9×9 mm², providing a capacitance of 25-30 pF at the input of amplifier. The depletion thickness of the diodes was 500 µm. The cross section of fibres bundles corresponds to 30% of the photodiode area in the case of two bundles and 20% for three bundles. To compensate for the extra electronics noise a long shaping ($\tau_{RC-CR} = 35-40$ ns) was used. The noise was determined from rms of the pedestals and was found to be 139 MeV, 127 MeV, 127 MeV for the left, central and right readout channel respectively for tower 15. For tower 16, a noise of 178 MeV and 172 MeV was measured for the left and the right channels respectively. If the appropriate size photodiode had been used, the noise would be reduced at the level of 80 MeV per channel for a shaping of 30 ns duration at the baseline [7,8], which fits the LHC requirements and would improve the calorimeter performance.

5. Experimental data and analysis

5.1. Channels inter-calibration

The average responses of multi-bundle tower channels are shown in Fig. 3 for a transversal scan of the tower with a 40 GeV electron beam. In the case of the two bundles tower, calibration requires that the integral response of each channel over the tower transversal coordinate are equal. After each channel inter-calibration the tower is calibrated as the whole.

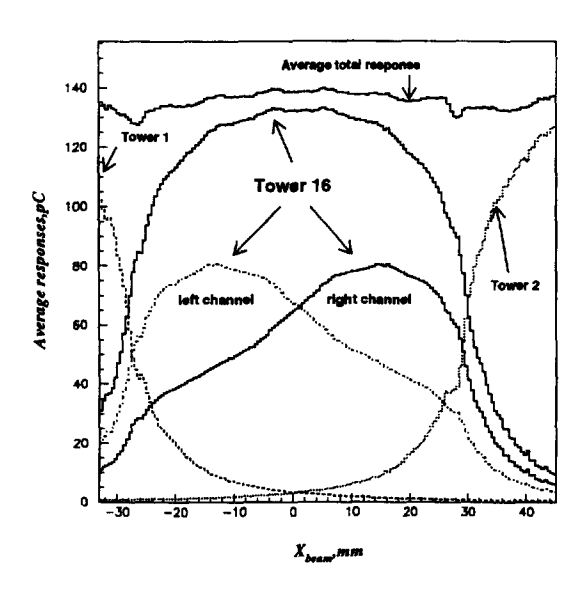
For the three bundles tower the left and the right channels are inter-calibrated by the same method. For the central channel response, it can be tuned to minimize the lateral nonuniformity of the tower.

We found that the energy resolution at the tower center is practically independent on the choice of calibration coefficient for the central channel. The dependence of energy resolution for an area of 7×7 mm² around the center of the tower on the calibration coefficient of central channel is shown on Fig. 4. The unity value of the central channel calibration coefficient corresponds to the optimal lateral uniformity of the total energy response.

The total response after calibration is also shown in Fig. 4. A good uniformity of the response is achieved.

5.2. Shower spatial resolution

The electromagnetic shower coordinate in a calorimeter can be determined from the center of gravity of the response of adjacent towers. In general the amplitude of the response of each calorimeter tower should be fitted to the shower shape. The cross talk between readout channels in the case of a multi-bundle tower leads to a distortion of the shower shape. This makes the analysis of spatial resolution more complicated than for a towers with a



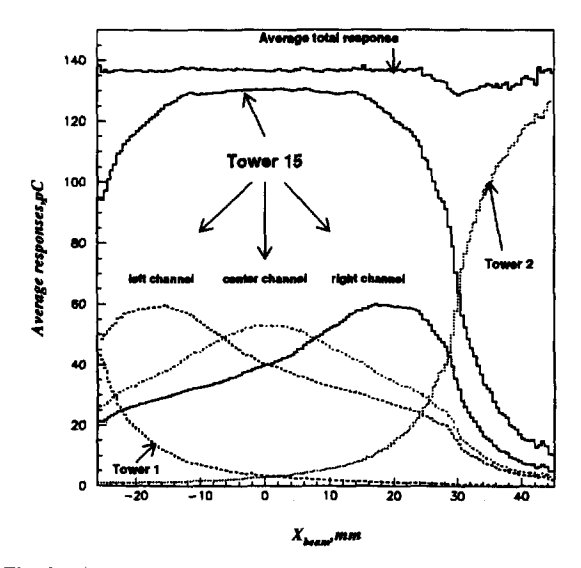
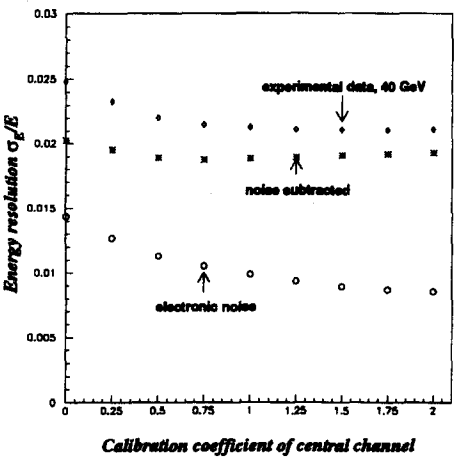


Fig. 3. The average responses of multi-bundle shashlik towers vs x_{beam} coordinate. The data around fibres are corrected in the scan of the tower with 3 channels.



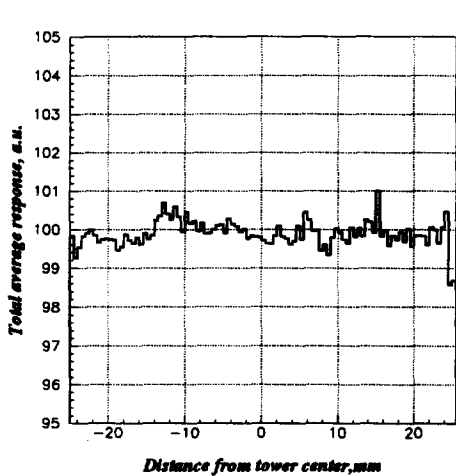


Fig. 4. (up) Energy resolution for the setup of Fig. 2 with a three-bundle tower a the center. It is a weak function of the calibration coefficient of the central channel. The central channel gain was adjusted to minimize the total lateral nonuniformity. (bottom) The total average response in a three-bundle shashlik tower vs x_{beam} coordinate for the calibration coefficient of central channel equal to 1.0. The data around fibres are corrected.

single readout. To simplify the analysis we studied the spatial resolution using the amplitude difference taken two by two.

5.2.1. Spatial resolution of the tower with two readout channels

Four amplitudes: $E_{\rm tower1}$, $E_{\rm tower2}$ and $E_{\rm left}$, $E_{\rm right}$ for tower 1, tower 2, left and right channels of tower 16 are measured (Fig. 2). Imposing the energy independence of the algorithm, one has to find three independent variables that determine the position of the impact. An almost optimal choice consists of the following functions:

At the center of tower 16 we will use:

$$x_1 = f_1((E_{\text{right}} - E_{\text{left}}) / (E_{\text{right}} + E_{\text{left}})).$$

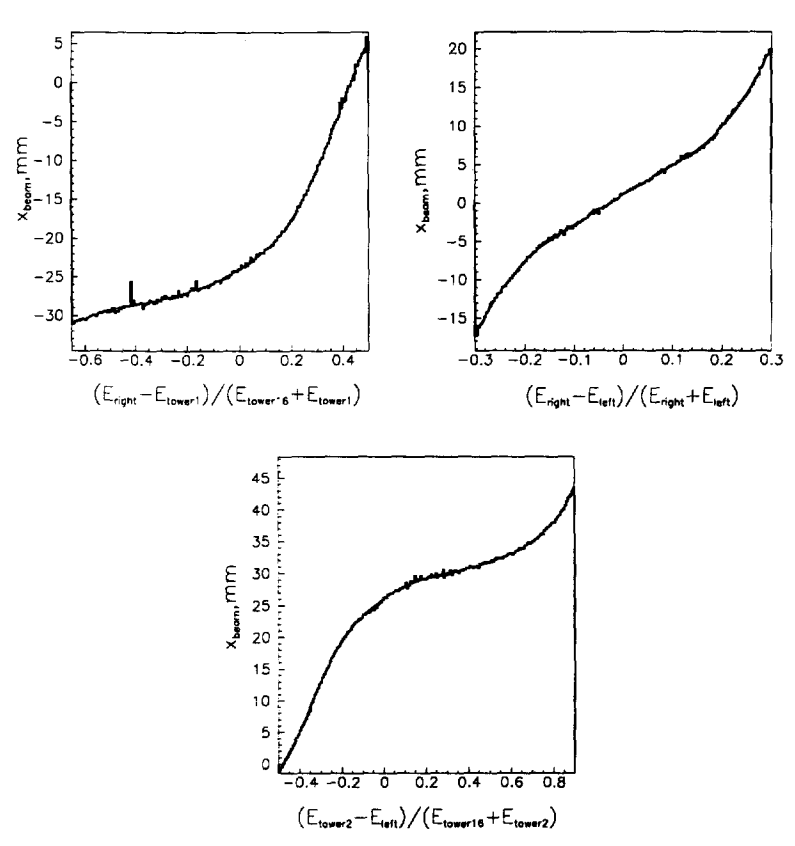


Fig. 5. The dependence of electron coordinate x_{beam} vs the value of the functions expressed in term of channels' amplitudes. The experimental points were fitted by an 8th degree polynom.

In the region between tower 1 and tower 16:

$$x_2 = f_2((E_{\text{right}} - E_{\text{tower1}}) / (E_{\text{tower1}} + E_{\text{tower16}})).$$

In the region between tower 2 and tower 16:

$$x_3 = f_3((E_{\text{tower2}} - E_{\text{left}})/(E_{\text{tower2}} + E_{\text{tower16}})).$$

These functions are shown in Fig. 5. The coordinate resolutions when each of these functions was used separately are shown in Fig. 6. Taking the optimal combination of x_1 , x_2 , x_3 one obtains the position resolution as shown in Fig. 7. The mean resolution for the scanned region is $830 \pm 140 \ \mu m$.

The electronic noise contribution to the spatial resolution is given by the dashed line in Fig. 7a. Its mean contribution to the space resolution is 330 μ m. It was obtained by smearing the average response, at a given position, with the electronic noise estimated from the measured pedestals.

The contribution of calorimeter itself to the spatial resolution is shown in Fig. 7b after unfolding of the electronics noise and beam chamber resolution (300 μm). The mean value for the spatial resolution improves to $690\pm125~\mu m$.

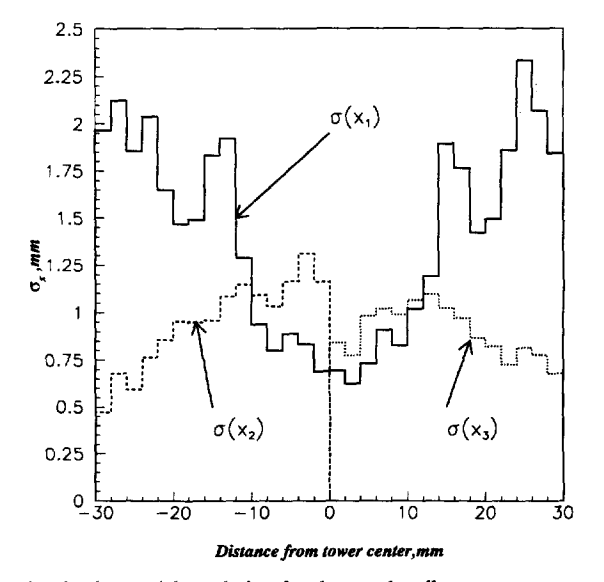


Fig. 6. The spatial resolution for the two bundle tower vs x_{beam} coordinate for functions f_1 , f_2 , f_3 used separately. $x_{\text{beam}} = 0$ at the center of the tower.

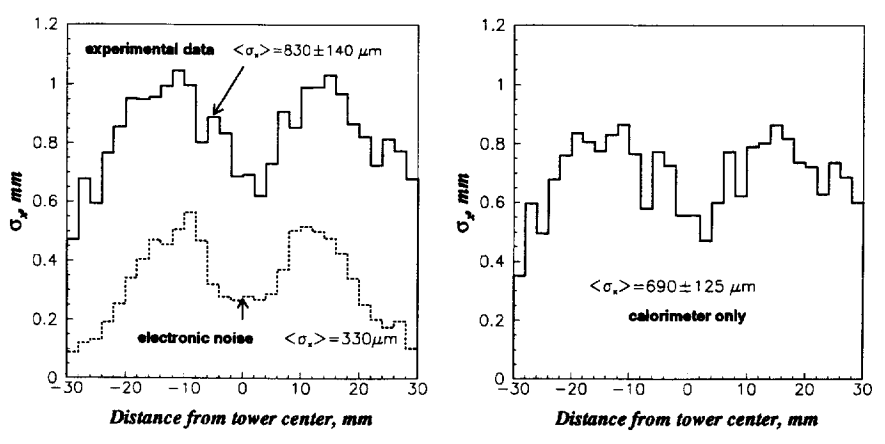


Fig. 7. The spatial resolution in the two bundle tower vs x_{beam} coordinate. Left plot: measured resolution, dashed line: electronics noise contribution, taken from pedestal measurement, right plot: resolution of calorimeter after unfolding of noise and beam chamber contributions.

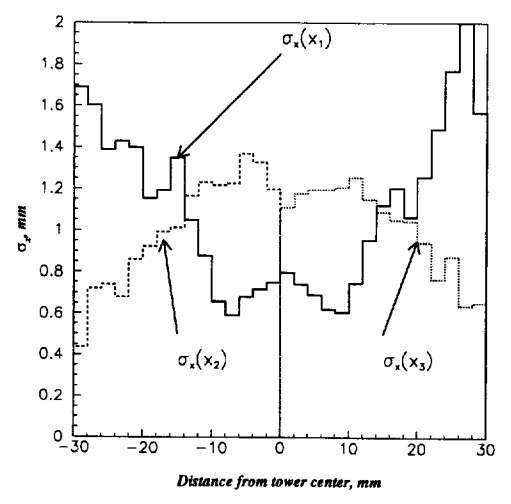


Fig. 8. The contributions of functions f_1 , f_2 , f_3 to the spatial resolution in the three channels tower vs x_{beam} coordinate.

5.2.2. Spatial resolution of the tower with three readout channels

To study the spatial resolution in a 3-bundle tower we used, in analogy with the case of two bundle tower, three functions f_1 , f_2 , f_3 depending on the channel amplitudes and four additional functions f_{2a} , f_{3a} , f_4 , f_5 :
At the center of tower 15:

$$x_1 = f_1((E_{\text{right}} - E_{\text{left}}) / E_{\text{tower15}}).$$

In the region between tower 1 and tower 15.

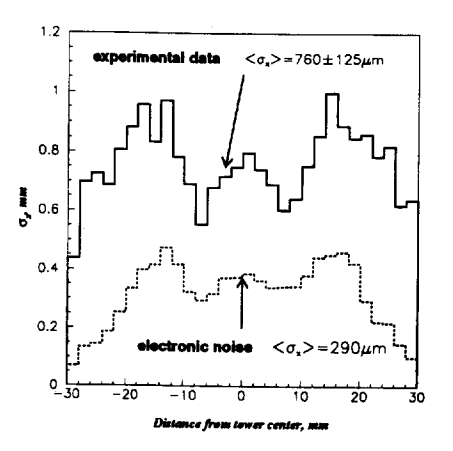
$$x_2 = f_2 \left(\left(E_{\text{right}} - E_{\text{tower1}} \right) / \left(E_{\text{tower1}} + E_{\text{tower15}} \right) \right),$$

$$x_{2a} = f_{2a} \left(\left(E_{\text{center}} - E_{\text{tower1}} \right) / \left(E_{\text{tower1}} + E_{\text{tower15}} \right) \right).$$

In the region between tower 2 and tower 15:

$$x_3 = f_3((E_{\text{tower2}} - E_{\text{left}})/(E_{\text{tower2}} + E_{\text{tower15}})),$$

$$x_{3a} = f_{3a}((E_{\text{tower2}} - E_{\text{center}})/(E_{\text{tower2}} + E_{\text{tower15}})).$$



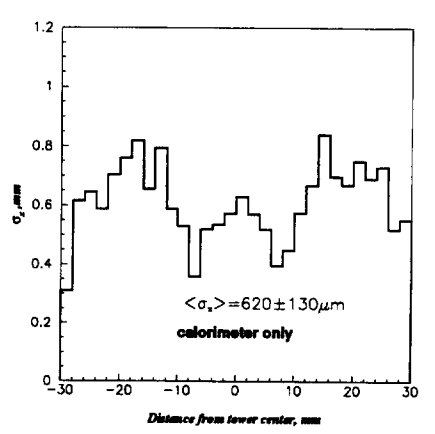


Fig. 9. Optimized spatial resolution for the three channels tower vs x_{beam} coordinate. Left plot: measured resolution, dashed line: electronics noise contribution, right plot: resolution of calorimeter after noise and beam chamber contributions have been unfolded.

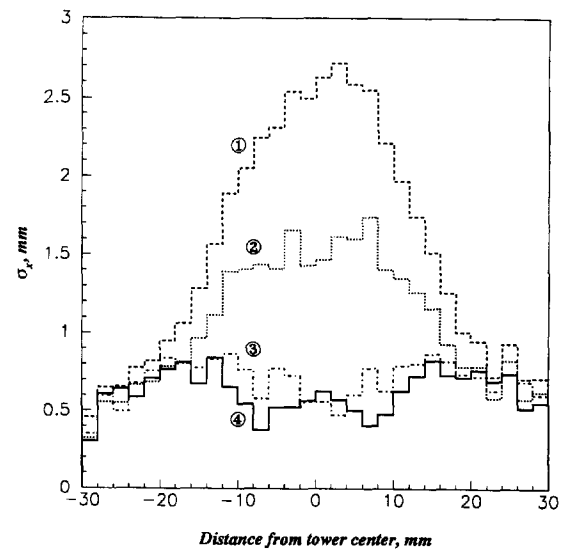


Fig. 10. Spatial resolution vs x_{beam} coordinate. (1) Resolution in tower with 2 channels if only the sum of amplitudes is used (identically to the tower with single channel readout). (2) The same as (1), but after unfolding of the electronics noise and beam chamber contributions. (3) Two bundle tower resolution. (4) Three bundle tower resolution.

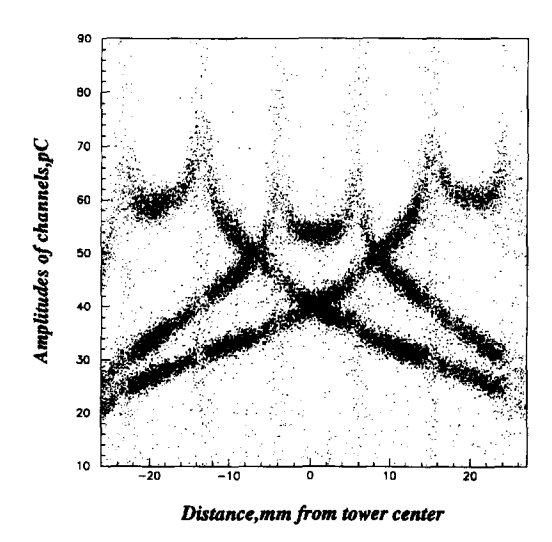


Fig. 11. Response of the three readout channels in tower 15 when a fibres region of ± 1.5 mm is used. Responses of the 3 channels are superimposed.

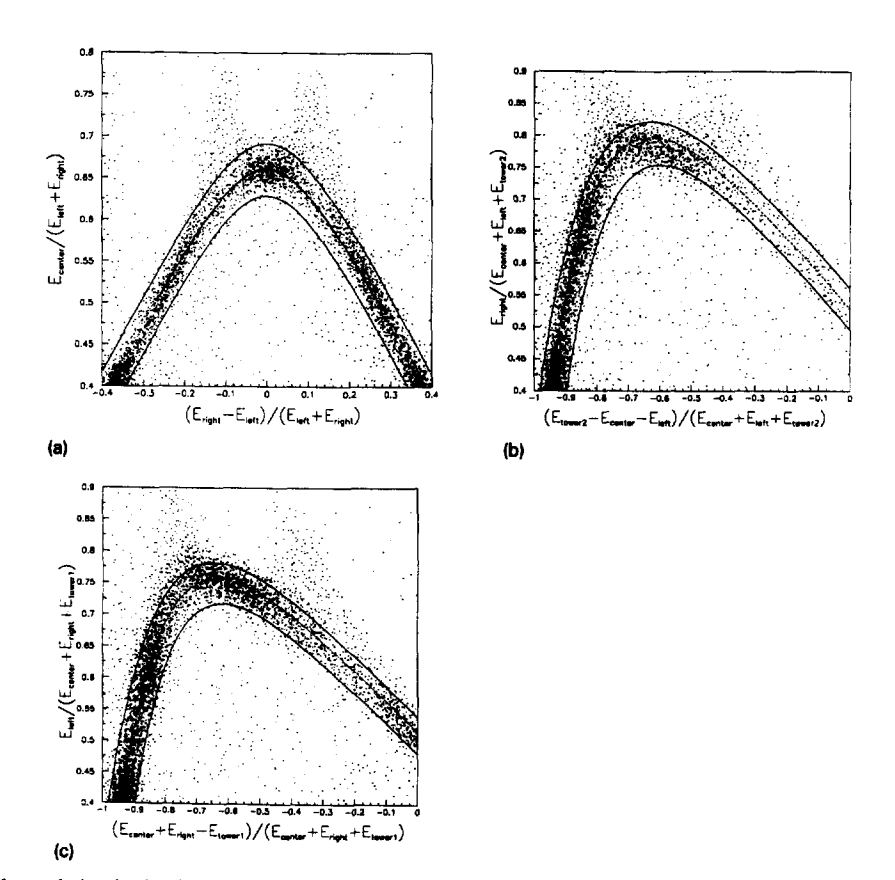


Fig. 12. The signal correlation in the three-bundle tower. The data outside the boundaries, such as data around fibres or charged particles hitting the photodiode might be either rejected or corrected. (a) Central channel, (b) right channel, (c) left channel.

In the region between central and left channels of tower 15:

$$x_4 = f_4 ((E_{\text{center}} - E_{\text{left}}) / E_{\text{tower15}}).$$

In the region between central and right channels of tower 15:

$$x_5 = f_5((E_{\text{right}} - E_{\text{center}})/E_{\text{tower15}}).$$

Fig. 8 shows the shower position resolution which can be achieved with f_1 , f_2 , f_3 functions. One can improve it by combining all the seven functions. Unfortunately, the values of these last functions are not independent, and, in practice, the optimal resolution is obtained using x_1 , x_2 , x_3 , and only slightly improves by the use of the four others.

The optimized resolution is shown in Fig. 9a. Its mean value over the scanned region is equal to $760\pm125~\mu m$. The dashed curve shows the electronics noise contribution. The resolution after the removal of electronics noise and beam chambers is shown on Fig. 9b. Its mean value is $620\pm130~\mu m$.

The improvement in the spatial resolution achieved with multi-bundle tower readout is shown in Fig. 10. For comparison the resolution obtained for a single-bundle tower with and without electronics noise is also shown.

5.3. Self-correction of fibre effect in multi-bundle tower

A large variation is observed when the electrons impact a W.L.S. fibre. Fig. 11 shows the variation of the amplitude of each channel of tower 15 versus the horizontal coordinate (x_{beam}) . The response of the channel which contains the fibre is distorted. For the same shower, the signal in the other channels is not perturbed allowing the possibility for correction. For instance, to correct the re-

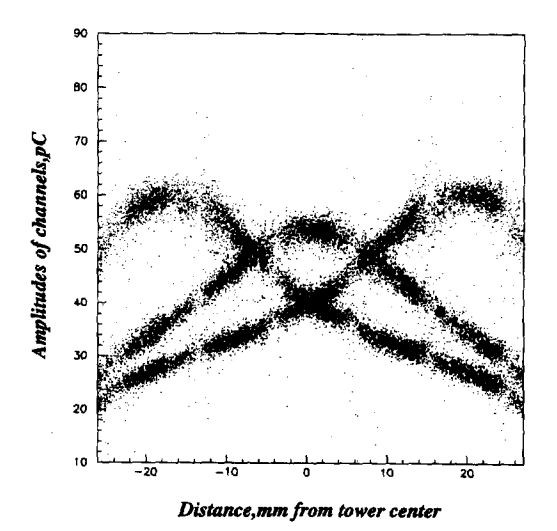
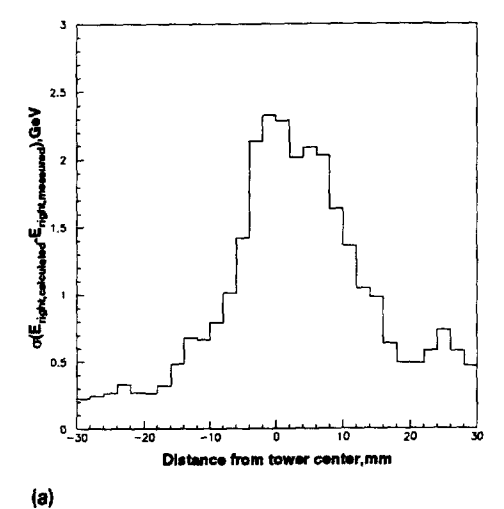


Fig. 13. The response of the three bundle tower in the fibres' regions after correction.



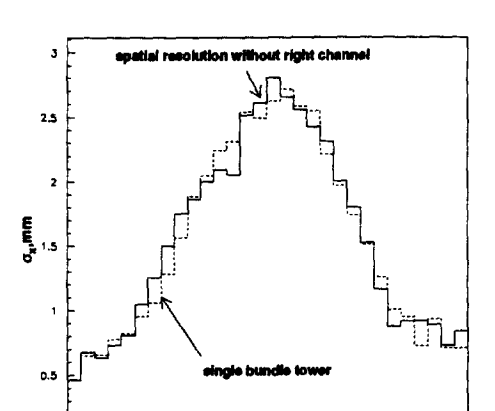


Fig. 14. (a) The precision of restoring the right channel response in the tower with two readout channels. (b) The spatial resolution in the tower with two channels, when the right channel information is not used. The dashed histogram represents the response of a single bundle tower.

(b)

sponse of the central channel we plot in (Fig. 12a) the ratio $E_{\rm center}/(E_{\rm left}+E_{\rm right})$ versus the asymmetry of the response of the left and right channels $(E_{\rm right}-E_{\rm left})/(E_{\rm left}+E_{\rm right})$. The fibre effect is clearly seen there. The corrected response for the central channel can be given by:

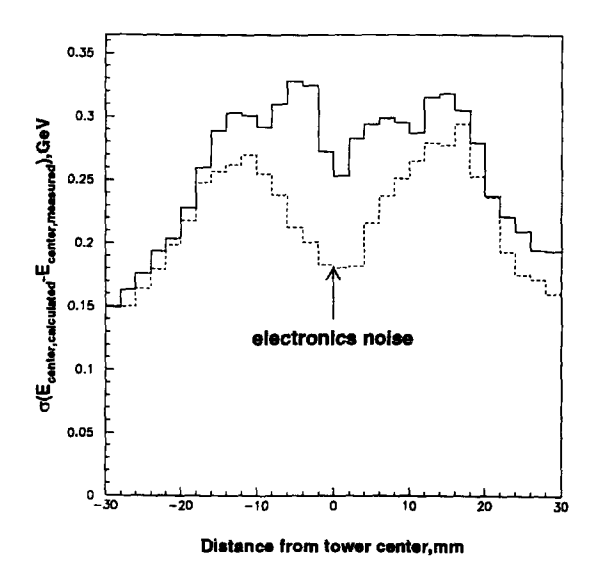
$$\begin{split} E_{\text{central, corrected}} &= \left(E_{\text{left}} + E_{\text{right}} \right) \times f_{\text{corr.}} \left(\left(E_{\text{right}} - E_{\text{left}} \right) \right. \\ & \left. / \left(E_{\text{left}} + E_{\text{right}} \right) \right). \end{split}$$

The correction function $f_{\rm corr.}$ and the boundaries of "good" events region are defined by selecting events that have electron impacts between two horizontal rows of fibres. The correction functions are defined by the shower shape

and by the light collection conditions. They are almost independent of the shower energy: the transversal shower profile being almost independent of the shower energy. The correlation plots for the right and left channels are shown in Fig. 12b and Fig. 12c. The right and left channels responses were corrected by the same method. The corrected channel responses are shown in Fig. 13. This procedure improves the energy resolution without event loss.

5.4. Recovery of dead channel

If the correlation functions defined above are known, a dead channel can be restored by the use of the other



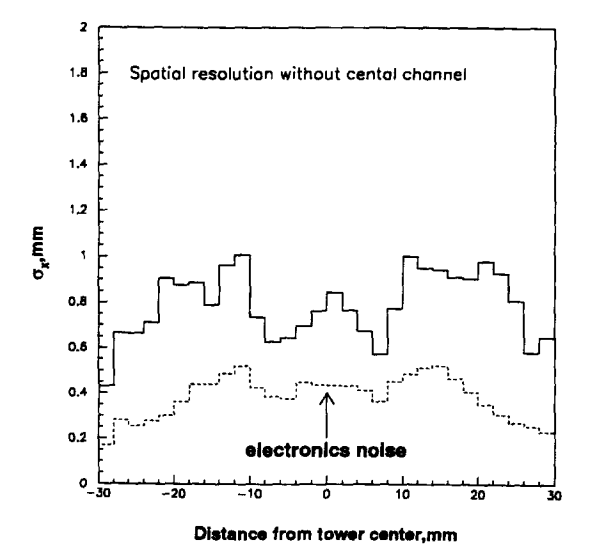
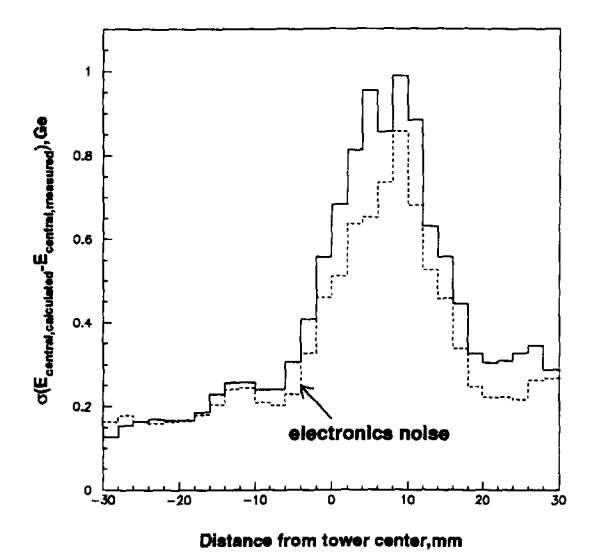


Fig. 15. The precision of restoring the central channel response in the tower with three readout channels and the spatial resolution without central channel signal use.



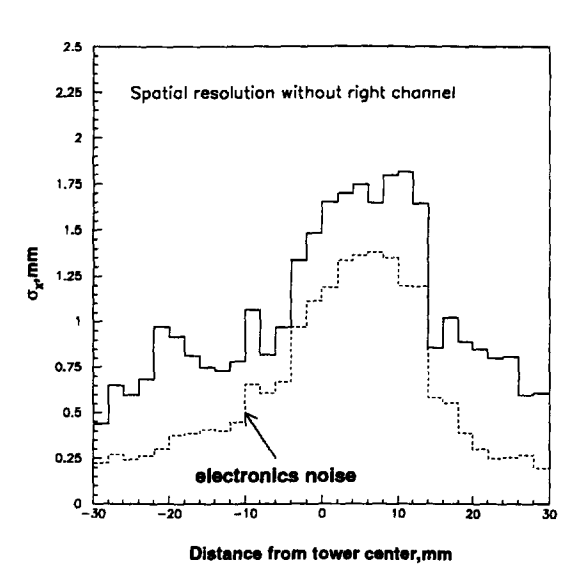


Fig. 16. The precision of restoring the right channel response in the tower with three channels. The spatial resolution without using the right channel.

signals. This improves the lifetime and reliability of the calorimeter, what is important for experiments at LHC which will have a duration of over 10 years. We have studied the precision of restoring a channel and the calorimeter performance achievable when the response of one channel is missing.

In the case of two-bundle tower, to restore for instance the right channel signal, we use the left channel signal and the signal of tower 2. The precision of restoring the right channel signal is shown in Fig. 14a. As it will be shown here after, the recovered response is mostly dominated by the electronics noise. The spatial resolution in the two-bundle tower (right channel not used) is shown in Fig. 14. It is practically the same as for a single-bundle tower.

In the case of three bundle tower we found that the central channel signal can be restored by using the left and the right channels data with a precision shown in Fig. 15a. We found that the spatial and energy resolution remain practically the same as when all channels function properly (see Figs. 15 and 17). The performance with the right channel signal not used is shown in Figs. 16 and 17. We see that the precision of restoration of the response of a channel is mainly dominated by the electronics noise.

5.5. Two showers separation

We studied the possibility of two showers separation in the three bundle tower. To separate the events consisting of two 40 GeV electron showers we used the correlation defined for the "fibre" effect correction. We simulated a two showers event by taking the sum of two single shower responses. So the electronics noise was also taken twice. The separation efficiency as function of the distance be-

tween the center of gravity of the two showers is shown in Fig. 18. The efficiency of single shower event selection for the same cuts was larger than 98%.

6. Conclusions

We studied prototypes of two- and three-bundle projective towers with 40 GeV electrons to examine the performance of a "shashlik" calorimeter that can be achieved with a multi-bundle design approach. Our experimental results at 40 GeV show that:

- the spatial resolution at the tower center in multibundle towers is improved by a factor of 2 to 3 in comparison with the same type of tower equipped with a single channel readout. In the region of the tower center the resolution with three bundles is better than with two bundles.
 - the lateral uniformity of the energy response in the

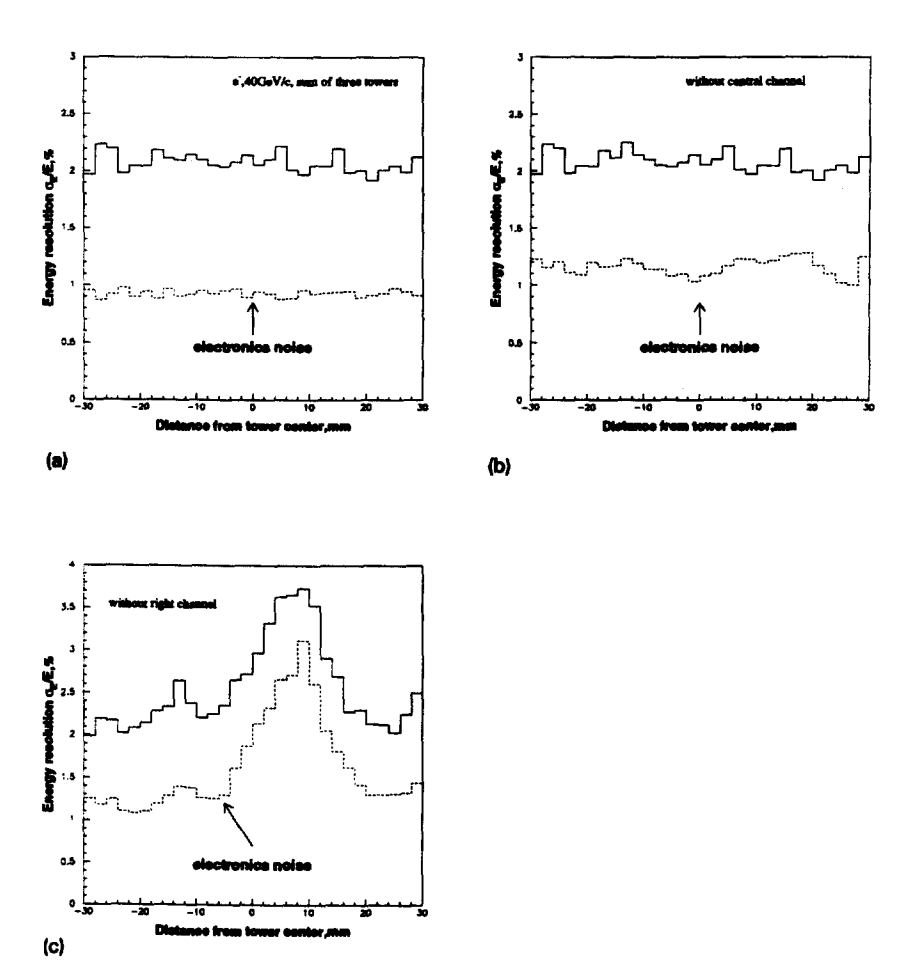


Fig. 17. (a) The energy resolution in the tower with three readout channels. The energy deposited in the three towers setup was about 92% of the total shower energy. (b) Energy resolution when the central channel response is not used but restored from right and left channels. (c) The same when the right channel is not used. The beam chamber information is not used in both cases. The dashed lines show the electronics noise contribution.

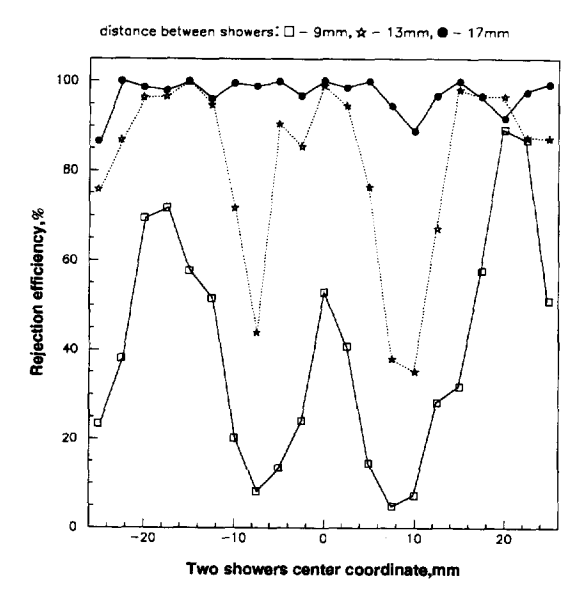


Fig. 18. The rejection efficiency of double shower events in the three bundle tower.

tower with three bundles is improved in comparison with two and one bundle cases. Excluding the region at tower edges (± 4.0 mm) where the total response is affected by the shower leakage, the uniformity of the response is better than 1%.

- the correlation of channel responses in a multi-bundle tower provides a possibility to correct the calorimeter response in the vicinity of fibres as well as the signal due to charged particles hitting the Si-photodiode at the rear of the tower. The correction is much more effective for the three bundle tower.
- the reliability due to the redundancy as well as the performance of a calorimeter are improved by multi-bundle tower design.
- two showers separation is also improved in multibundle towers.

- all the performances mentioned above were mainly limited by electronics noise.

A study of the calibration of three bundle towers is in progress.

The use of multi-bundle towers leads to larger size towers. This will improve the calorimeter hermeticity and lower its cost. We conclude that a multi-bundle design is a good choice for a shashlik type calorimeter.

Acknowledgements

We would like to thank all engineers and technicians from the collaboration laboratories and more specifically V. Shmatkov from INR that have been involved in the work described in this note. The data were taken with the RD5 DAQ and beam setup and we are grateful to our colleagues from RD5 and in particular G. Bencze, F. Szoncso and C. Wulz who made our running conditions possible and easy. Finally, we are grateful to the SPS staff and in particular N. Doble for providing assistance in understanding the beam line during tests.

References

- [1] CMS Letter of Intent, CERN/LHCC 92, October 1992.
- [2] CMS Status Report and Milestones, CERN/LHCC 93-48, October 1993, CERN/LHCC 94-20, May 1994.
- [3] H. Fessler et al., Nucl. Instr. and Meth. A 228 (1985) 303; and Nucl. Instr. and Meth. A 240 (1985) 284;
 - B. Loher et al., Nucl. Instr. and Meth. A 254 (1987) 26;
- G.S. Atoyan et al., Nucl. Instr. and Meth. A 320 (1992) 144.[4] J. Badier et al., CERN-CMS TN/93-66, INR-821/93,X-
- LPNHE/93-4(1993) Nucl. Instr. and Meth. A 348 (1994) 74.
- [5] E. Guschin, Yu. Musienko, I. Semenjuk, INR-856/94 preprint.
- [6] J. Badier et al., CERN-CMS TN/93-108.
- [7] E. Guschin et al., CERN-CMS TN/93-108.
- [8] A. Karar, CERN-CMS TN/93-96 (1993); and Proc. 4th Int. Conf. on Calorimetery in High Energy Physics, La Biodala, Isola d'Elba, Italy, 1993, eds. A Menzione and A. Scribeno (World Scientific).